HiSST: 3rd International Conference on
High-Speed Vehicle Science Technology
14 -19 April 2024, Busan, Korea

Extension of the lean blow-off limit in the scramjet combustor by the multi-channel gliding arc plasma

Rong Feng[1], Zhipeng Meng[2], Jiajian Zhu[3*], Bo Wang[4], Mingbo Sun[5], Xiaoqing Chen[6], Chao Ding[7]*

Abstract

A multi-channel gliding arc (MCGA) plasma is utilized to extend the lean blow-off limit of the cavity shear-layer flame in the scramjet combustor. Optical measurements including high-speed flame chemiluminescence, high-speed CH*emissions, and high-speed schlieren are used to characterize the reaction zone coupled with the flow field assisted by the plasma. The results show that the lean blow-off limit of the cavity shear-layer flame is extended by 21% when the MCGA plasma is added. The flame is blown out eventually due to a small amount of heat release near the lean blow-off limit. While the plasma is applied, the plasma can sustain the flame in the whole combustion process. The center of the flame tends to be concentrated near the plasma region, indicating that the flame is more likely to attach to the MCGA plasma. The heat release of the mainstream flame is strengthened by the MCGA plasma to prevent extinguished. A plausible mechanism for the extension of the lean blow-off limit is revealed that the temperature is enhanced by the heat and active radicals produced by the MCGA plasma, which sustain the flame near the plasma region. Subsequently, the small flakes of the flame spread to the half back of the cavity to form the global flame with approximate local conditions.

Keywords: *Scramjet combustor, Lean blow-off limit, Gliding arc plasma, Cavity shear-layer flame*

Nomenclature

Multi-channel gliding arc – MCGA

Global Equivalence Ratio – GER

dielectric barrier discharge – DBD

Excited state of nitrogen – N_2*

Hydrogen atom – H

1. Introduction

The applications of non-equilibrium plasma-assisted supersonic combustion have attracted much attention in last decades [1, 2]. Non-equilibrium plasma has a lower temperature than equilibrium plasma, whereas it has a higher electron temperature and better chemical selectivity [3]. The non-equilibrium plasma avoids excessive heating of neutral particles, and its external electric field energy

[1] *National innovation institute of defense technology, No. 53 East Street, Haidian District, Beijing, rongfeng@nudt.edu.cn*
[2] *National innovation institute of defense technology, No. 53 East Street, Haidian District, Beijing, 1066598335@qq.com*
[3] *National University of Defense Technology, No. 109 Deya street, jjzhu@nudt.edu.cn*
[4] *National innovation institute of defense technology, No. 53 East Street, Haidian District, Beijing, bowang@nudt.edu.cn*
[5] *National University of Defense Technology, No. 109 Deya street, sunmingbo@nudt.edu.cn*
[6] *National innovation institute of defense technology, No. 53 East Street, Haidian District, Beijing, 969629728@qq.com*
[7] *National innovation institute of defense technology, No. 53 East Street, Haidian District, Beijing, 368409679@qq.com*

can be effectively used to produce a large number of high-energy electrons, radicals, and other components with high chemical reactivity [4], which can change the chemical reaction path and increase the reaction rate [5, 6].

Typical non-equilibrium plasmas include dielectric barrier discharge (DBD) plasma [7, 8], nanosecond pulsed plasma [9, 10], gliding arc plasma [11-13], and microwave plasma [14, 15]. Matsubara et al. [16] integrated a plasma torch and DBD plasma to assist hydrogen flame in a supersonic flow. The wall pressure increases significantly after the application of DBD plasma, while the discharge power of DBD is only 8 W. Nanosecond pulsed plasma is characterized by the rising edge of the pulse discharge with nanoseconds, so there is little heat accumulation during the discharge process [17]. Do et al. [18] applied nanosecond pulsed discharge in the supersonic flow, and the area of the OH signal was significantly enhanced. The supersonic combustion is strengthened through using low-power microwaves by Meng Yu et al. [19].

Gliding arc plasma can produce a large number of high-energy electrons [20, 21]. Meng et al. [22] combined the gliding arc and microwave in the supersonic flow. When the gliding arc is applied, the heat release region is moved forward with higher combustion efficiency. Thus, the gliding arc plasma has potential to be used in the scramjet combustor. The MCGA plasma is created by our group with more discharge area [23]. The MCGA plasma can increase the combustion intensity [24], and it can stabilize the flame in unstable conditions [25].

Although the application of non-equilibrium plasma strengthen combustion stability in the scramjet combustor has been investigated in recent years [26], the extension of the lean blow-off limit in the scramjet combustor by the gliding arc plasma was rarely reported. In this paper, the MCGA plasma is utilized to extend the lean blow-off limit in the scramjet combustor. High-speed CH*emissions, high-speed photography, and high-speed schlieren are used to visualize the process. A plausible mechanism for the extension of the lean blow-off limit by the MCGA is proposed.

2. Experimental setup

The direct-connect test was conducted at the NUDT (Ma2.92 inflow, 1 kg/s) [27, 28]. The configurations of the combustor are shown in Fig. 1. The breakdown distance of the gliding arc is 11 mm. An injector with a diameter of 2 mm is put in front of the cavity leading edge with 70 mm to inject the ethylene fuel.

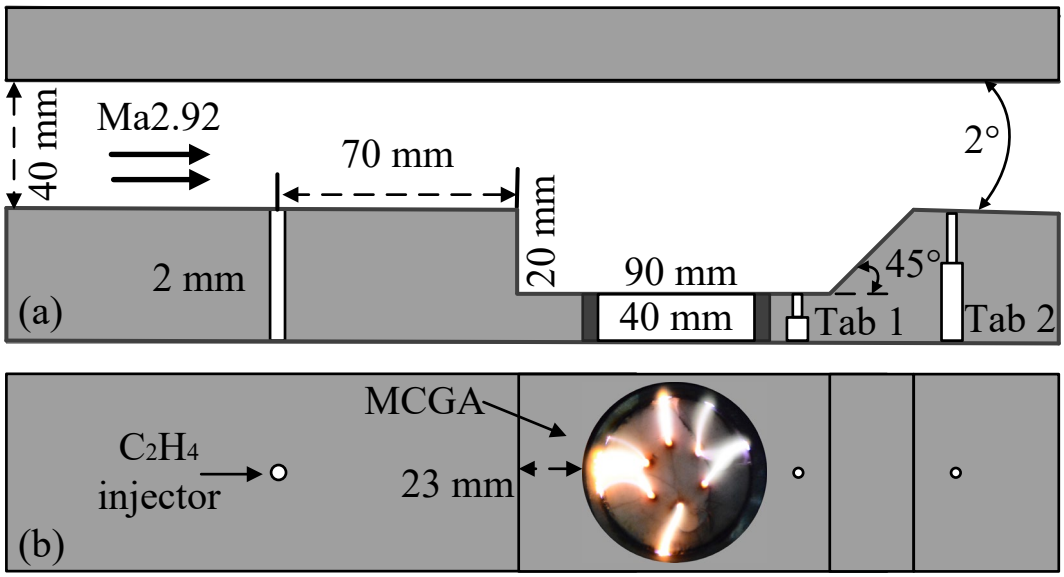

Fig 1. The configuration of the scramjet combustor.

Diagnostic equipment of the direct-connect tests are displayed in Fig. 2. Simultaneous high-speed schlieren (10kHz, 1μs) and high-speed camera (10kHz, 98μs) are employed to characterize the flow field coupled with the reaction zone assisted by the gliding arc plasma. High-speed CH* emission (20kHz, 49μs) and current/voltage probes are utilized to visualize the detailed combustion process and measure

the power consumed by the plasma generator.

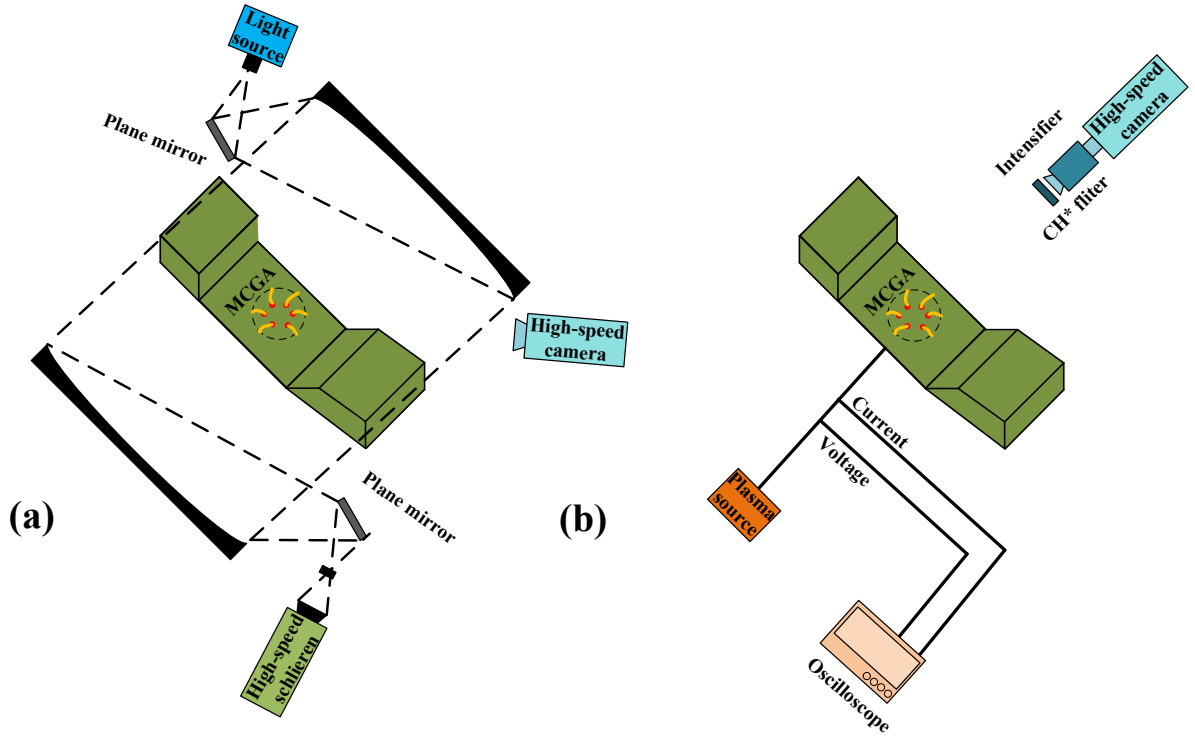

Fig 2. Diagnostic equipment of the experiment.

The time sequence of the test is displayed in Fig. 3(a). The ethylene fuel is injected for 1150 ms in the whole experiment process. For comparison, the plasma works for 285 ms first, then it turns off for 450 ms, and it works for 396 ms at last. The average power is about 6000W, which is calculated by the current and voltage waveforms. The MCGA discharge belongs to the spark-type mode [29, 30], which exists multiple current spikes in the waveforms.

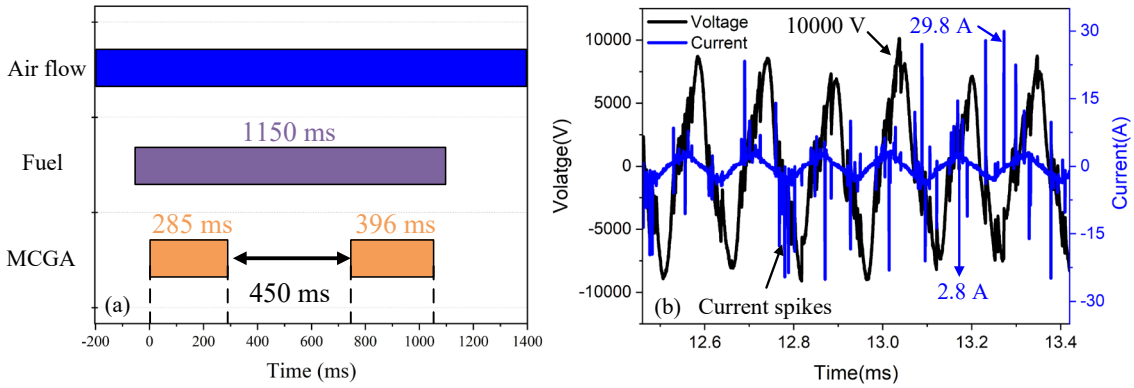

Fig 3. Time sequence of the test (a) and the waveforms of the MCGA (b).

The detailed cases are shown in Table 1. Each case is repeated two times. When the GER is larger than 0.19, the flame can be merely held by the cavity in the whole process. When the GERs are equal to 0.15 and 0.17, the flame is unable to be kept without the plasma whenever the flame can be kept with the plasma. When the GERs are equal to 0.13, the poor flame can be partially held by the plasma. It can be inferred that the lean blow-off limit of the flame is 0.19, and the plasma extends to 0.15, indicating that the lean blow-off limit of the supersonic combustion is extended by 21% when the MCGA plasma is added.

Table 1. Typical cases.

Case	GER	State
Case 1	0.13	Partially held by the MCGA
Case 2	0.15	Completely held by the MCGA
Case 3	0.17	Completely held by the MCGA
Case 4	0.19	Held by the cavity
Case 5	0.22	Held by the cavity

3. Results and discussion

Fig. 4 shows the typical blown out process with or without the MCGA. The flame is ignited by the MCGA successfully at t=2561 ms. However, when the plasma is off, the flame is unable to be maintained by the cavity. From t=4064ms to t=4073ms, the flame is more concentrated in the middle of the cavity accompanied by the disappearance of the original flame. At t=4073ms, the flame is extinguished eventually due to the strong turbulence, as seen in the corresponding schlieren imaging.

Once the plasma is on, the global flame can be re-ignited, as seen in Fig. 4 at t= 7966 ms. It is noteworthy that the plasma can entirely hold the combustion until the fuel jet is off. From t=8058 ms to t=8061 ms, the cavity flame is unstable and is nearly blown out. However, the flame is attached near the plasma at t=8061 ms which is hard to be extinguished due to the heat and the radicals provided by the plasma. The flame fragment tends to develop to the global flame at t=8067 ms, which is stabilized by the plasma. Meanwhile, the MCGA plasma continuously produces the new flame kernel supply to the cavity flame [31], which is also beneficial to maintain the combustion. In the schlieren imaging, the area of the cavity shear-layer is larger than the state without the plasma, indicating that the heat release of the reaction zone is more stable.

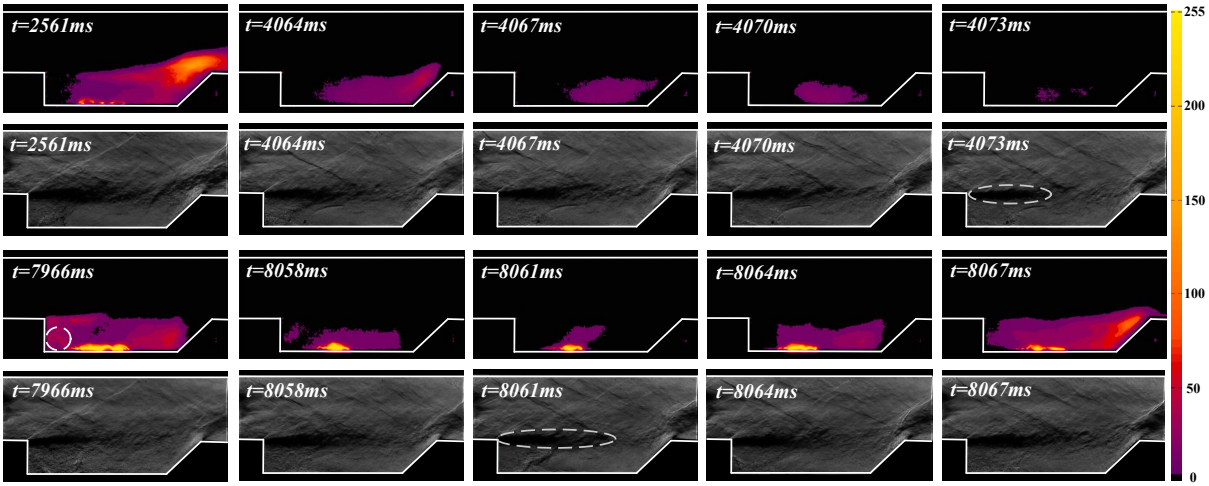

Fig 4. Simultaneous images of high-speed schlieren and photography in Case 3.

20 kHz high-speed CH* emissions is used to characterize the reaction zone to calculate the normalized area. Fig. 5 shows the wall pressure and the normalized area along with time. The positions of pressure tabs are displayed in Fig. 1. The flame is completely sustained until the MCGA plasma is off at t=290 ms. The flame is completely extinguished after the plasma is off for nearly 43 ms, acompanished by the pressure decrease. When the MCGA is added, the flame can be re-ignited immediately, and it can be held entirely by the plasma until the fuel jet is off for 390 ms. The pressure distributions and the area variation indicate that the plasma can strengthen the flame stability near the lean blow-off limit, leading to the flame held by the plasma.

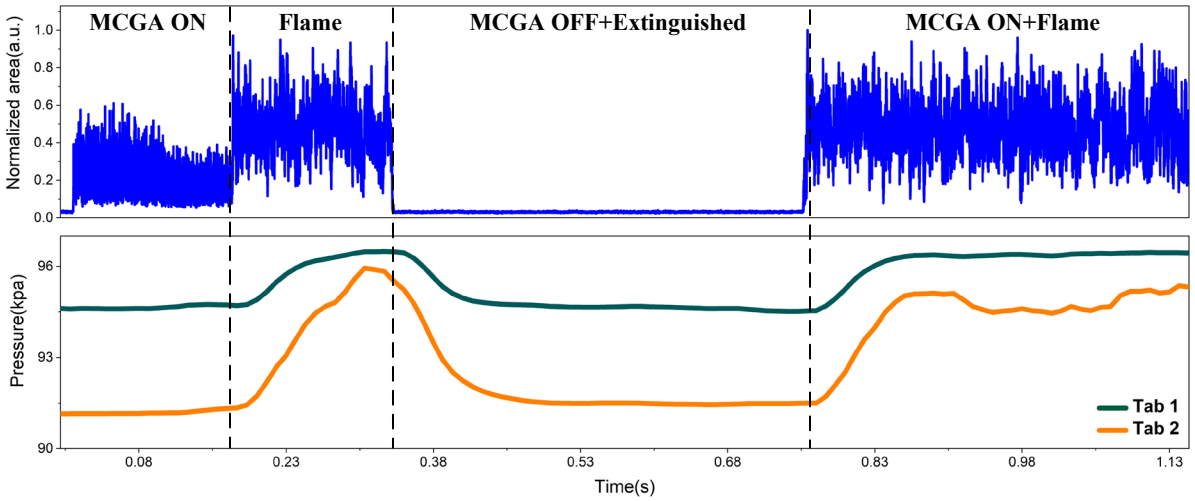

Fig 5. The wall pressure and the normalized area vary with time in Case 2.

The detailed combustion process assisted by the plasma can be observed below. The time interval of the sequence images is 50 μs. From t=0 μs to t=150 μs, the cavity flame is gradually extinguished due to the less fuel. The flame is nearly blown out at t=200 μs located near the cavity ramp. However, at t=250 μs, the flame spreads forward from the ramp of the cavity, and it gradually attaches to the plasma at t=400 μs. The flame is strengthened by the plasma to prevent extinguished, which is held near the MCGA plasma and stretches to the back half of the cavity. At t=550 μs, the flame is filled in the cavity to develop to the global flame.

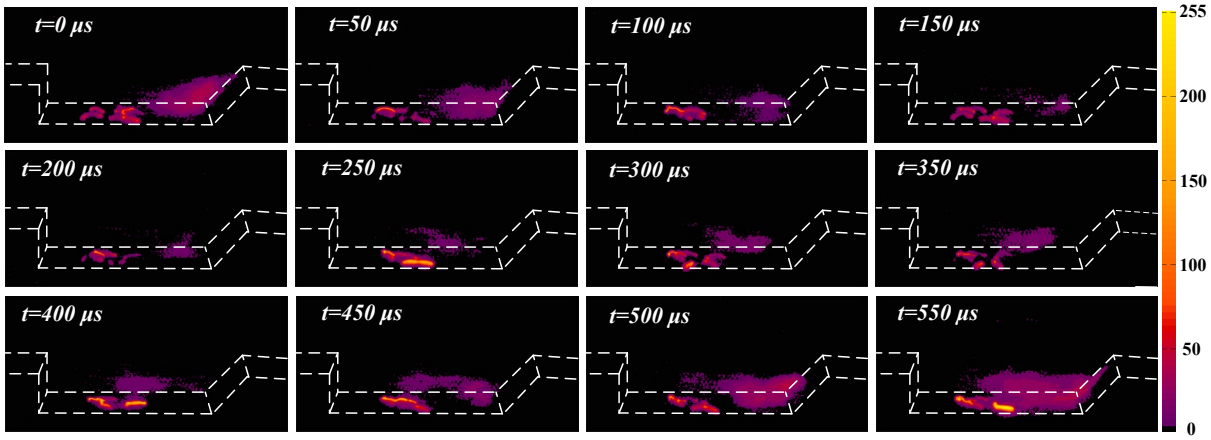

Fig 6. The detailed combustion process assisted by the MCGA plasma in Case 2.

The combustion oscillation process can be represented by the center point of the flame. The distribution of the flame center point with or without the plasma is shown below. At the CH* emission images, the pixels regarded as the flame are extracted firstly, and the coordinate of the flame center point is taken as the average value of pixels on the x-axis and y-axis. Moreover, the value of the plasma area is regarded as 0 to avoid interfering with the result. About 14000 images are calculated to form the flame center distribution in Fig. 7. In Fig. 7(a), the flame center points are mostly concentrated near the cavity ramp caused by the combustion mode of the cavity-shear layer. From Fig. 7(b), it can be found that part of the flame center points tend to be concentrated near the MCGA plasma, indicating that the flame is more likely to attach to the plasma [32].

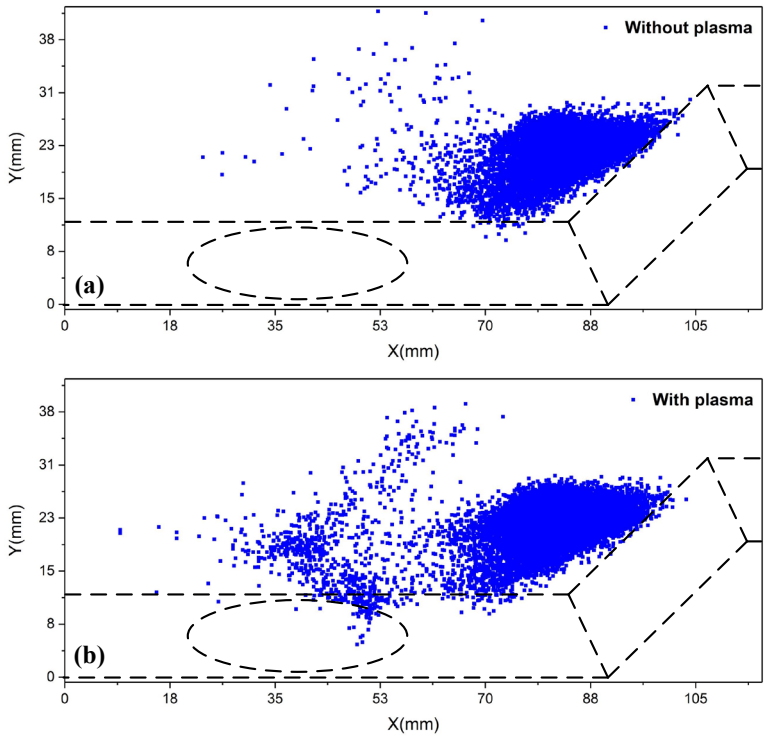

Fig 7. The scatter distribution of the flame center point with 14000 images. (a) without the MCGA. (b) with the MCGA.

The time-averaged images of the CH* emissions in three equivalence ratios are shown in Fig. 8. Each image is averaged from 1000 instantaneous images, and the divided image is obtained from the time-averaged images with the plasma divided by the time-averaged images without the plasma. It is noteworthy that the time-averaged intensity is strengthened with the plasma due to the stronger exchange of the heat and radicals in the cavity. According to the divided images, the strengthened area is basically concentrated in the mainstream, which can reach 1.6 times. It can be inferred that the heat and radical transform in the cavity is enhanced by the MCGA plasma [33], leading to higher combustion intensity with more heat release in the mainstream.

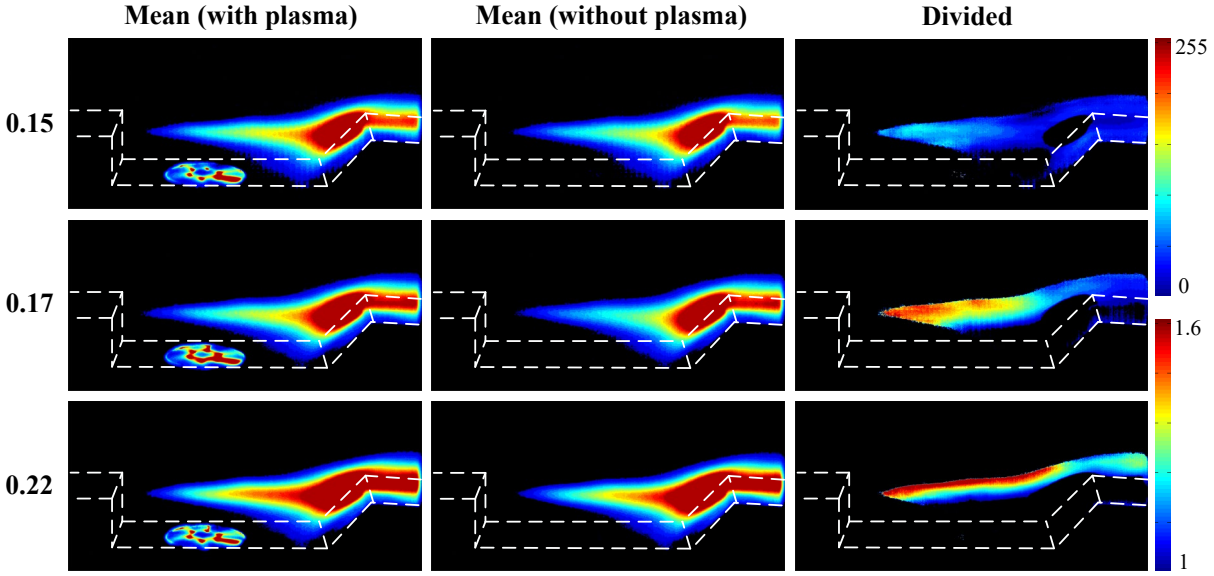

Fig 8. The time-averaged images and the divided images of the flame CH* emissions in three different equivalence ratios.

A plausible mechanism for the extension of the lean blow-off limit by the MCGA is proposed. In the

absence of the plasma, when the global equivalence ratio exceeds the lean blow-off limit, the flame is blown out eventually due to a small amount of heat release while the small flakes of the flame exist near the cavity ramp, as can be observed in Fig. 9(a). The small flakes of the flame are stretched by the turbulence and the heat release is unable to ignite the fresh fuel continuously.

In the presence of the plasma, when the ratio of the fuel/air mixture is less, the flame still tends to be separated into small flakes of the flame. However, the small flakes of the flame can propagate to the plasma region, which is held by the increased temperature and the active radicals (N_2^*, H) produced by the MCGA plasma [26, 34]. Then, it spreads to the half back of the cavity to form the stable cavity-shear layer flame with suitable turbulence conditions and approximate local equivalence ratios [35]. The shear-layer is also strengthened by the plasma and the cavity flame with the backward shock wave in the flow field. Meanwhile, the heat and chemical effects of the MCGA plasma strengthen the heat and radical transform in the cavity, which leads to a stable mainstream flame.

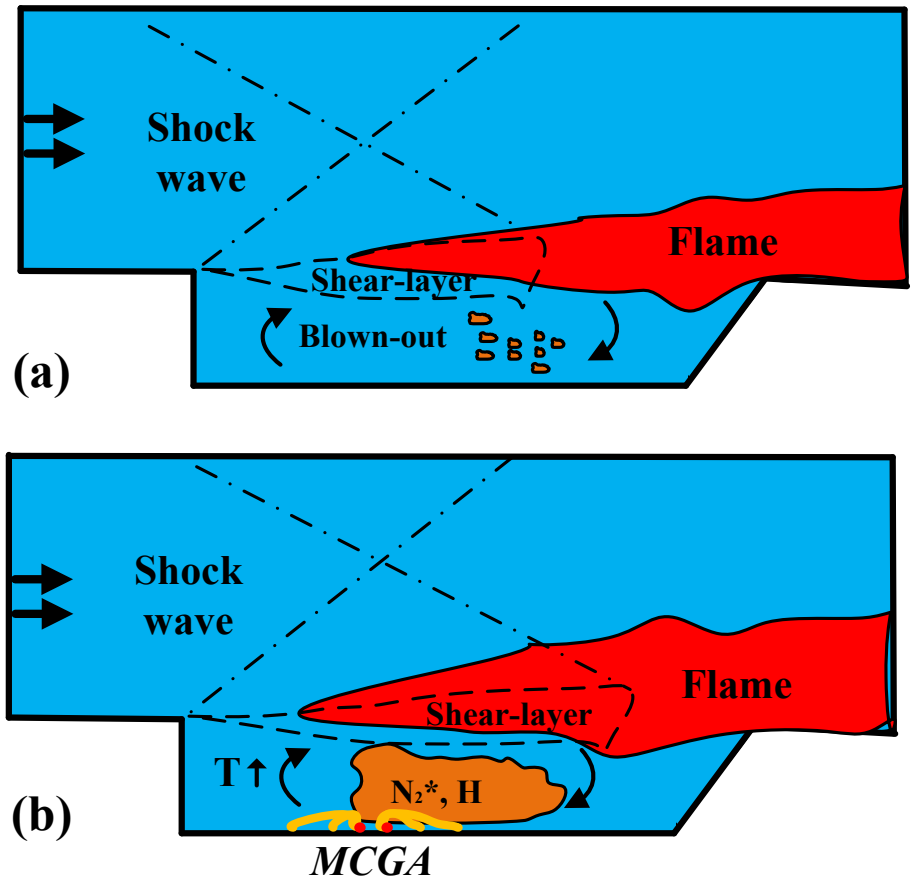

Fig 9. Mechanism sketches for the extension of the lean blow-off limit by the MCGA plasma. (a) Without the plasma. (b) With the plasma.

4. Conclusions

In conclusion, a multi-channel gliding arc plasma is used to extend the lean blow-off limit in the scramjet combustor. Simultaneous high-speed schlieren (10kHz) and high-speed camera (10kHz), high-speed CH* emission (20kHz), and current/voltage probes are used to characterize the flow field, the reaction zone, and the discharge state. The detailed points are listed below.

1. The MCGA discharge in the cavity belongs to the spark-type mode with 6000W, which exists multiple current spikes in the waveforms.
2. The lean blow-off limit in the scramjet combustor is extended by 21% when the MCGA plasma is added. The flame can be held entirely by the plasma until the fuel jet is off.
3. The flame center points tend to be concentrated near the plasma region, indicating that the flame is tend to attach to the MCGA discharge. The intensity of the mainstream flame is strengthened by

the MCGA to prevent extinguished.

4. In the absence of the plasma, when the global equivalence ratio exceeds the lean blow-off limit, the flame is blown out eventually due to a small amount of heat release. In the presence of the plasma, the small flakes of the flame are held by the increased temperature and the active radicals (N_2^*, H) produced by the plasma, which develops to the global flame with approximately local conditions.

References

1. A. Starikovskiy, N. Aleksandrov, Plasma-assisted ignition and combustion, Progress in Energy and Combustion Science, 39 (2013) 61-110.
2. T.M. Ombrello, S.D. Hammack, C.D. Carter, K. Busby, J.K. Lefkowitz, Scramjet cavity ignition using nanosecond-pulsed high-frequency discharges, Combustion and Flame, 262 (2024) 113335.
3. Y. Ju, W. Sun, Plasma assisted combustion: Dynamics and chemistry, Progress in Energy and Combustion Science, 48 (2015) 21-83.
4. Y. Ju, W. Sun, Plasma assisted combustion: Progress, challenges, and opportunities, Combustion and Flame, 162 (2015) 529-532.
5. Y. Ban, S. Zhong, J. Zhu, F. Zhang, Effects of non-equilibrium plasma and equilibrium discharge on low-temperature combustion in lean propane/air mixtures, Fuel, 339 (2023) 127353.
6. L. Cheng, N. Barleon, B. Cuenot, O. Vermorel, A. Bourdon, Plasma assisted combustion of methane-air mixtures: Validation and reduction, Combustion and Flame, 240 (2022) 111990.
7. J. Deng, P. Wang, Y. Sun, J. Zhou, Y. Luo, D. He, Design and experimental investigation of a dual swirl combined DBD plasma combustor head actuator, Sensors and Actuators A: Physical, 344 (2022) 113707.
8. L. Massa, J.B. Freund, Plasma-combustion coupling in a dielectric-barrier discharge actuated fuel jet, Combustion and Flame, 184 (2017) 208-232.
9. T.S. Taneja, P.N. Johnson, S. Yang, Nanosecond pulsed plasma assisted combustion of ammonia-air mixtures: Effects on ignition delays and NOx emission, Combustion and Flame, 245 (2022) 112327.
10. M. Shahsavari, A.A. Konnov, A. Valera-Medina, M. Jangi, On nanosecond plasma-assisted ammonia combustion: Effects of pulse and mixture properties, Combustion and Flame, 245 (2022) 112368.
11. Y. Tang, D. Xie, B. Shi, N. Wang, S. Li, Flammability enhancement of swirling ammonia/air combustion using AC powered gliding arc discharges, Fuel, 313 (2022) 122674.
12. C. Kong, J. Gao, J. Zhu, A. Ehn, M. Aldén, Z. Li, Re-igniting the afterglow plasma column of an AC powered gliding arc discharge in atmospheric-pressure air, Applied Physics Letters, 112 (2018).
13. J. Zhu, J. Gao, A. Ehn, M. Aldén, Z. Li, D. Moseev, Y. Kusano, M. Salewski, A. Alpers, P. Gritzmann, M. Schwenk, Measurements of 3D slip velocities and plasma column lengths of a gliding arc discharge, Applied Physics Letters, 106 (2015).
14. L. He, Y. Zhang, H. Zeng, B. Zhao, Research progress of microwave plasma ignition and assisted combustion, Chinese Journal of Aeronautics, 36 (2023) 53-76.
15. J. Hwang, C. Bae, J. Park, W. Choe, J. Cha, S. Woo, Microwave-assisted plasma ignition in a constant volume combustion chamber, Combustion and Flame, 167 (2016) 86-96.
16. Y. Matsubara, K. Takita, G. Masuya, Combustion enhancement in a supersonic flow by simultaneous operation of DBD and plasma jet, Proceedings of the Combustion Institute, 34 (2013) 3287-3294.

17. X. Wang, Y. Gao, S. Zhang, H. Sun, J. Li, T. Shao, Nanosecond pulsed plasma assisted dry reforming of CH4: The effect of plasma operating parameters, Applied Energy, 243 (2019) 132-144.

18. H. Do, M.A. Cappelli, M.G. Mungal, Plasma assisted cavity flame ignition in supersonic flows, Combustion and Flame, 157 (2010) 1783-1794.

19. Y. Meng, H. Gu, X. Zhang, Influence of microwave on structure of supersonic combustion flame, Acta Aeronautica et Astronautica Sinica, 40 (2019).

20. J. Zhu, J. Gao, A. Ehn, M. Aldén, A. Larsson, Y. Kusano, Z. Li, Spatiotemporally resolved characteristics of a gliding arc discharge in a turbulent air flow at atmospheric pressure, Physics of Plasmas, 24 (2017).

21. J. Zhu, J. Gao, Z. Li, A. Ehn, M. Aldén, A. Larsson, Y. Kusano, Sustained diffusive alternating current gliding arc discharge in atmospheric pressure air, Applied Physics Letters, 105 (2014).

22. Y. Meng, H. Gu, W. Sun, X. Zhang, Microwave enhanced gliding arc plasma assisted supersonic combustion, Acta Aeronautica et Astronautica Sinica, 41 (2020).

23. Y. Tian, J. Zhu, M. Sun, H. Wang, Y. Huang, R. Feng, B. Yan, Y. Sun, Z. Cai, Enhancement of blowout limit in a Mach 2.92 cavity-based scramjet combustor by a gliding arc discharge, Proceedings of the Combustion Institute, 39 (2023) 5697-5705.

24. R. Feng, Y. Huang, J. Zhu, Z. Wang, M. Sun, H. Wang, Z. Cai, Ignition and combustion enhancement in a cavity-based supersonic combustor by a multi-channel gliding arc plasma, Experimental Thermal and Fluid Science, 120 (2021) 110248.

25. R. Feng, M. Sun, H. Wang, Y. Huang, Y. Tian, C. Wang, X. Liu, J. Zhu, Z. Wang, Experimental investigation of flameholding in a cavity-based scramjet combustor by a multi-channel gliding arc, Aerospace Science and Technology, 121 (2022) 107381.

26. R. Feng, J. Zhu, Z. Wang, F. Zhang, Y. Ban, G. Zhao, Y. Tian, C. Wang, H. Wang, Z. Cai, M. Sun, Suppression of combustion mode transitions in a hydrogen-fueled scramjet combustor by a multi-channel gliding arc plasma, Combustion and Flame, 237 (2022) 111843.

27. B. An, Z. Wang, L. Yang, X. Li, C. Liu, The ignition characteristics of the close dual-point laser ignition in a cavity based scramjet combustor, Experimental Thermal and Fluid Science, 101 (2019) 136-140.

28. Q. Li, J. Zhu, Y. Tian, M. Sun, M. Wan, B. Yan, T. Luo, Y. Sun, C. Wang, T. Tang, H. Wang, Investigation of ignition and flame propagation in an axisymmetric supersonic combustor with laser-induced plasma, Physics of Fluids, 35 (2023).

29. R. Feng, J. Zhu, Z. Wang, M. Sun, S. Zhong, F. Zhang, Discharge characteristics of a gliding arc discharge in a supersonic jet air flow, Physics of Plasmas, 29 (2022).

30. J. Zhu, Z. Sun, Z. Li, A. Ehn, M. Aldén, M. Salewski, F. Leipold, Y. Kusano, Dynamics, OH distributions and UV emission of a gliding arc at various flow-rates investigated by optical measurements, Journal of Physics D: Applied Physics, 47 (2014) 295203.

31. R. Feng, J. Zhu, Z. Wang, M. Sun, H. Wang, Z. Cai, B. An, L. Li, Ignition modes of a cavity-based scramjet combustor by a gliding arc plasma, Energy, 214 (2021) 118875.

32. R. Feng, J. Zhu, D. Li, Z. Meng, M. Sun, H. Wang, C. Wang, C. Wang, Z. Wang, Characteristics of the flame flashback in a dual-mode scramjet combustor by the gliding arc plasma, Applications in Energy and Combustion Science, 14 (2023) 100143.

33. G. Choubey, Y. Devarajan, W. Huang, K. Mehar, M. Tiwari, K.M. Pandey, Recent advances in cavity-based scramjet engine- a brief review, International Journal of Hydrogen Energy, 44 (2019) 13895-13909.

34. R. Feng, Z. Meng, J. Zhu, M. Sun, H. Wang, Y. Yang, C. Wang, F. Zhang, Y. Ban, B. Yan, C. Wang, X. Liu, Z. Wang, Gliding Arc Plasma-Controlled Behaviors of Jet-Wake Stabilized Combustion in a Scramjet Combustor, AIAA Journal, 61 (2023) 2789-2798.

35. R. Feng, Z. Wang, M. Sun, H. Wang, Y. Huang, Y. Yang, X. Liu, C. Wang, Y. Tian, T. Luo, J. Zhu, Multi-channel gliding arc plasma-assisted ignition in a kerosene-fueled model scramjet engine, Aerospace Science and Technology, 126 (2022) 107606.